# Orbits of Minor Bodies of the Solar System in the Circular Restricted Three-Body Problem

Jeremy B Tatum* and Mandyam N Anandaram †

## Abstract

A brief introduction to the circular restricted three-body problem (CR3BP) is given where a third body of negligible mass moves under the combined gravitational-centrifugal potential of two co-rotating massive bodies restricted to circular orbits. The equipotential contours of a variety of two body systems in the solar system are presented along with interesting orbits of Trojans, Hildas, Thule in the Sun-Jupiter system, the *libration* of Pluto in the Sun-Neptune system and choreographic orbits.

**Keywords**: CR3BP, equipotential contours, orbits, Trojans, Hildas, Thule, Pluto, figure-of-eight orbits.

## 1. Introduction

The complete general motion of three massive bodies moving under their mutual gravitation cannot be expressed in terms of simple algebraic solutions; rather, the motions of the three bodies must in the most general case be calculated numerically. However, certain restricted versions of the problem are capable of relatively simple algebraic analysis. In one of the most celebrated restricted versions of three-body motion which has many applications in

* University of Victoria, British Columbia, Canada; jtatum@uvic.ca
†Bangalore University, Bangalore, India; mnanandaram@gmail.com

astronomy, two massive bodies are moving in circular orbits around their mutual centre of mass. If $M_1$ and $M_2$ are the two masses with a constant distance *a* between them then it is simple to show that the orbital angular speed $\omega$ is given by

$$\omega^2 = \frac{G(M_1 + M_2)}{a^3},$$

(1)

In the circular restricted three-body problem, a third body of negligible mass *m* is moving under the influence of these two bodies and in their orbital plane but it has no effect on their motion. The problem is to describe the motion of the third body relative to the two massive bodies. A well-known practical application is to determine the motion of the asteroids under the influence of the Sun and Jupiter. Another application is to consider the motion of clouds of gas that may be circulating in the vicinity of the two components of a binary star system. Yet another application is the placement of spacecraft at suitable locations around the Sun-Earth system or around the Earth-Moon system.

The motion of the third body is conveniently described by supposing it to move in the gravitational potential wells of the two massive bodies. The gravitational potential at a point that is at a distance $r_1$ from $M_1$ and $r_2$ from $M_2$ is

$$-G\left(\frac{M_1}{r_1} + \frac{M_2}{r_2}\right).$$

(2)

One can imagine this as being represented by two deep hyperboloidal wells.

However, for many purposes it is convenient to refer the motion of the third body relative to the two massive orbiting bodies; that is, to refer its motion to a coordinate system in which the two massive bodies are at rest. Such a coordinate system can be chosen so that its origin is at the centre of mass of $M_1$ and $M_2$, its *xy*-plane is in the orbital plane of $M_1$ and $M_2$, and these two masses are conveniently situated along the *x*-axis of this co-rotating system. Relative to inertial space, the coordinate system is rotating at angular speed $\omega$ given by equation (1) above. Consider now our third body of small

mass and whose motion is restricted to the orbital plane of the two massive bodies. Suppose at some time it is at a distance $r_1$ from $M_1$, $r_2$ from $M_2$, and $r$ from the centre of mass of $M_1$ and $M_2$. When referred to such a co-rotating coordinate system, this third body experiences not only the gravitational attraction of the two massive bodies, but it also experiences a centrifugal force $mr\omega^2$ flinging it (still in the orbital plane) away from the origin of coordinates. Like the gravitational force, the centrifugal force is a conservative force, and the centrifugal "field" $r\omega^2$ is derivable from a centrifugal potential function $-\frac{1}{2}r^2\omega^2$ (plus an arbitrary constant, which we can take to be zero).

Thus, when referred to this co-rotating frame, our third body moves, as it were, in a potential given by

$$-G\left(\frac{M_1}{r_1} + \frac{M_2}{r_2}\right) - \tfrac{1}{2}r^2\omega^2, \tag{3}$$

where $\omega$ is given by equation (1). This equipotential surface is illustrated in Figure 1. It can be thought of as a paraboloidal hill (that's the centrifugal part, $-\frac{1}{2}r^2\omega^2$) into which are sunk two deep hyperboloidal gravitational wells.  In Figure 2(a), we show a three dimensional solid model of this surface constructed at the departmental workshop of the University of Victoria. The three dots along center line from top to bottom are the collinear Lagrangian points and the two sideways across are the equilateral Lagrangian points.  Equation (3) can be re-written (with some effort) in x and y coordinates in the form

$$W(x, y) = -\frac{\mu_1}{\left((x+\mu_2)^2 + y^2\right)^{1/2}} - \frac{\mu_2}{\left((x-\mu_1)^2 + y^2\right)^{1/2}} - \frac{x^2 + y^2}{2}. \tag{4}$$

Here the symbols have the following meanings. $x$ and $y$ are coordinates of a point in units of the (constant) separation $a$ of the two massive bodies; $\mu_1 = M_1/M$ is the first primary mass ratio, $\mu_2 = M_2/M$ is the second primary mass ratio and $M = M_1 + M_2$ is the total
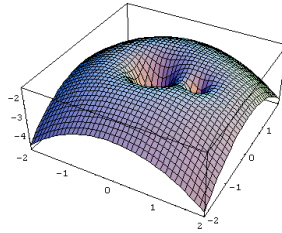
Fig.1. Equipotential surface plot in 3-D drawn by Maxwell Fairbairn using *Mathematica* software.
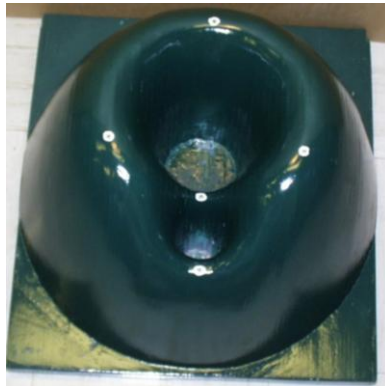


Fig. 2(a).  A 3-D model constructed by Mr. David Smith of  the University of Victoria.
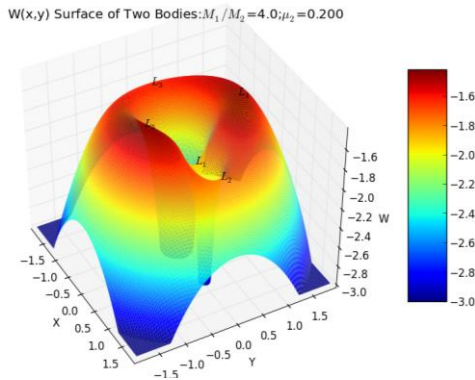


Fig. 2(b). This is a computer generated 3-D co-rotating equipotential surface  drawn for $\mu_2 = 0.2$.

mass of the two primaries; $W$ is the scaled gravitational-centrifugal potential in units of   $GM/a$.  The unit of time is given by $1/\omega$. Equation (4) is also referred to as the co-rotating potential. This equation is used to draw the equipotential contours shown in many

32

of the figures in this article. A computer generated contour surface drawn for the case of $\mu_2 = 0.2$ is shown in Figure 2(b). Here we can notice that the libration points $L_4$ and $L_5$ lie at potential maxima and the other three $L_1, L_2$ and $L_3$, lie lower at potential saddle like regions since the potential has values -1.420, -1.420, -1.599, -1.776 and -1.902 respectively at these points. Hence we find that $W(L_5) = W(L_4) > W(L_3) > W(L_2) > W(L_1)$ a result valid for all CR3B cases.

One way to imagine the trajectory of a third body of small mass, referred to the rotating reference frame and hence subject to the two gravitational forces and the centrifugal force, is to imagine a small particle sliding or rolling around on the surface shown in Figure 1. But this does not quite accurately describe the motion, because, whenever this particle moves, with a velocity **v** (referred to the rotating frame), it experiences yet another force, familiar to those who have studied classical mechanics, namely the *Coriolis force*, which is *at right angles* to its instantaneous velocity vector and *parallel to the plane of the orbits* of the two massive bodies. In particular, the Coriolis force is given in magnitude and direction by the equation

$$\mathbf{F} = 2m\mathbf{v} \times \boldsymbol{\omega} \tag{5}$$

Here the magnitude of $\boldsymbol{\omega}$ is given by equation (1), and its direction is normal to the plane of the orbits of the two massive bodies. This equation may remind us of the equation for the Lorenz force on a moving charged particle, of charge $Q$, in a magnetic field **B**, namely $\mathbf{F} = Q\mathbf{v} \times \mathbf{B}$. The analogy between $\boldsymbol{\omega}$ and **B** is evident. We cannot show the Coriolis force in Figures 1, 2(a) and 2(b), because it *cannot be derived from the gradient of a scalar potential*. But, like the magnetic field, it **can** be derived from the curl of a vector potential. We do not pursue that further here, since there may be danger in trying to push the analogy too far.

## 2. Co-rotating Equipotential Contours

It is useful to exhibit the co-rotating potential field in the form of co-rotating equipotential contours, as shown in Figure 3. We particularly draw attention to five points, known as the *Lagrangian points*, where the gradient of the potential is zero. They can be seen

in all the Figures 3 to 15. The distance scale used in these figures is such that one unit represents the constant distance between the two primaries $M_1$ and $M_2$. Three of the points, $L_1$, $L_2$ and $L_3$, known as the collinear Lagrangian points, are in the line joining $M_1$ and $M_2$, and their exact position depends upon the mass ratio $q = M_1/M_2$ or $\mu_2 = M_2/M$. The points $L_4$ and $L_5$ form an equilateral triangle each with $M_1$ and $M_2$, whatever the value of the mass ratio. These five points are *equilibrium points*, and, in principle a particle placed at any of these points would stay there, motionless in the rotating coordinate system. However, it was shown in Figure 2(b) that $L_4$ and $L_5$ are *maxima*, and $L_1$, $L_2$ and $L_3$ are *saddle points*, and therefore, contrary to the impression one is sometimes misled by, all five points are points of *unstable* equilibrium, and a particle situated at one of these points would rapidly fall away from it on the slightest disturbance [1]. We show in Figure 5 the orbital plane contour of the critical Roche lobe surface surrounding the two masses for two mass ratios. This is also a co-rotating equipotential contour corresponding to its value at the Lagrangian point $L_1$ where the two Roche lobes just touch each other. It is through this point in close binary stellar systems that the more massive star would begin to suffer a streaming mass loss to its smaller companion after its expanding atmosphere completely fills up the part of the Roche lobe surface surrounding it and then expands further beyond it.

Now, in the solar system, two massive bodies orbiting around their mutual centre of mass are the Sun and Jupiter. The mass of the Sun is more than a thousand times the mass of Jupiter, so the centre of mass of the system is well within the body of the Sun, so that at least to a first approximation it appears that Jupiter is revolving around the Sun even though the more accurate statement is that in the opening sentence of this paragraph. Those who are familiar with the asteroids will know that there is a class of asteroids known
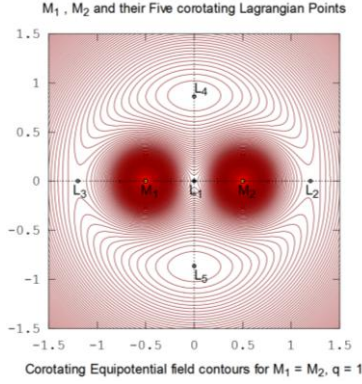
Fig. 3. The co-rotating equipotential contours are for the primary mass ratio $q = 1$ or $\mu_2 = 0.5$ .
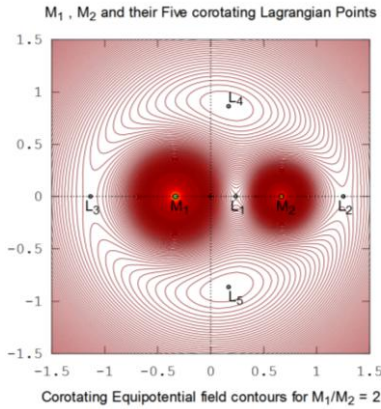


Fig. 4. The co-rotating equipotential contours are for the primary mass ratio $q = 2$ or $\mu_2 = 1/3$ .

as "Trojans", since they are named after heroes in the Trojan wars, and that they are orbiting around the Sun-Jupiter barycentre in the approximate vicinity of $L_4$ and $L_5$ – that is, they are in roughly the same orbit as Jupiter, but roughly 60° ahead of the planet or 60° behind the planet. Readers may also be aware of the *SOHO* spacecraft which is in orbit around the Sun roughly at the $L_1$ Lagrangian point of the Sun-Earth system which is about 1.5 million kilometers away from the Earth in the direction of the Sun. Since we have just stated that the Lagrangian points are points of *unstable* equilibrium, these circumstances are going to require some explanation!
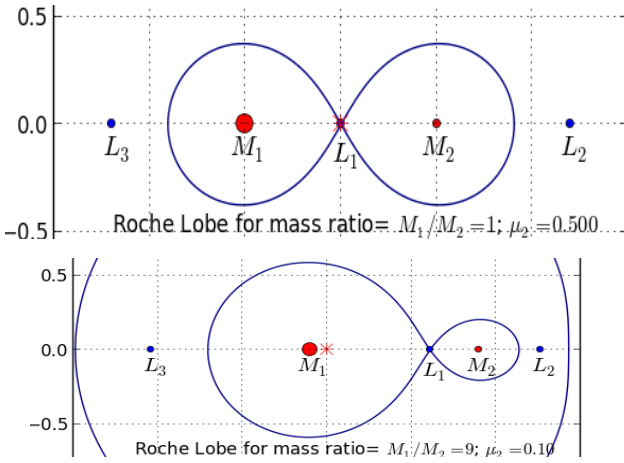
Fig. 5. The critical Roche Lobe is drawn for two mass ratios (1 and 9) as the co-rotating equipotential contour corresponding to a minor body potential at the collinear Lagrangian point $L_1$ calculated from Equation (4) in the text. The center of mass of the primaries is located at the origin (red X mark).
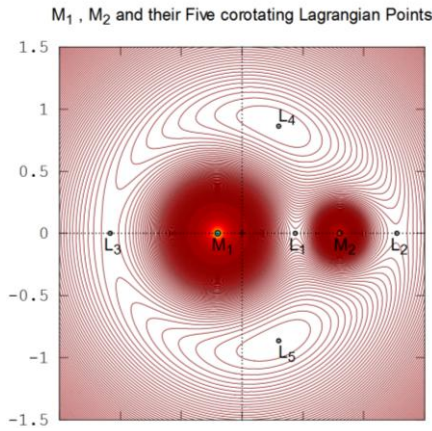


Fig. 6. The co-rotating equipotential contours are for the primary mass ratio $q = 4$ or $\mu_2 = 1/5$ .
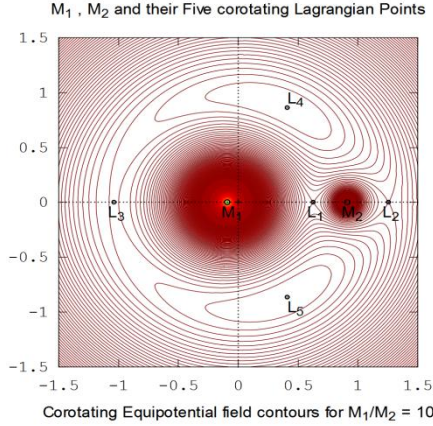
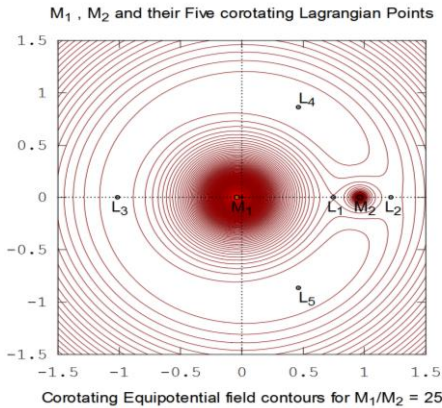Fig. 7. The co-rotating equipotential contours are for the primary mass ratio $q = 10$ or $\mu_2 = 1/11$ .



Fig. 8. The equipotential contours are for the primary mass ratio $q = 25$ or $\mu_2 = 1/26$. Notice here that as $q > 24.96$ or $\mu_2 < 1/25.96$ theoretical analysis indicates that for minor bodies of negligible mass **stable orbits** around the Lagrangian points are **just** possible in this system (see text).

As far as the Trojan asteroids are concerned, the explanation, qualitatively, is this. In the rotating reference frame, no Trojan is exactly *at* $L_4$ or $L_5$. Referred to the rotating frame, the asteroids are in the general vicinity of these points but are in clockwise orbit around them, in orbits that are not very dissimilar in shape to the equipotential curves of Figures 3 to 8. Imagine a small particle rolling clockwise around the summits of the potential hills at $L_4$ and $L_5$. As it moves around the hill is a clockwise direction, the *Coriolis force* tends to push it up the hill and prevents it from rolling

away. If the particle is in *counterclockwise* motion around L4 or L5, however, the Coriolis force will straightway send it rolling down the hill. So it is the Coriolis force that allows *stable orbits around L4 and L5*, although the points themselves are unstable.

Detailed analysis of the motion shows, however, that, in order for such orbits to be stable, the mass ratio $q = M_1/M_2$ must be greater than 24.9599358 (or, $\mu_2 = M_2/M$ must be less than 0.03852089). This exotic-looking number is actually $(25 + 3\sqrt{69})/2$, being a solution of the equation $q^2 - 25q + 1 = 0$ but we shall not derive that condition here. In any case, the condition is well-satisfied for the Sun-Jupiter system, for which $q = 1047.35$ or the Earth-Moon system for which q = 81.3. However, such stable orbits are not possible at a saddle point, such as L1. In order to keep the SOHO spacecraft in the vicinity of L1 a small hydrazine thrust is given to the spacecraft every three months or so. Similar is the case of GAIA spacecraft which has recently been positioned at the Sun-Earth Lagrangian point $L_2$ in order to carry out unobstructed astrometry of about a billion stars in our galaxy.

### 3. Orbits of Minor Bodies

We have computed a few interesting cases of particle orbits in the orbital plane of the two primary masses by integrating the expressions for its acceleration components given below using the same notation as well as scaling adopted in Equation(4):

$$\ddot{x} = x + 2\dot{y} - \frac{\mu_1(x+\mu_2)}{r_1^3} - \frac{\mu_2(x-\mu_1)}{r_2^3} \qquad (6)$$

$$\ddot{y} = y - 2\dot{x} - \frac{\mu_1 y}{r_1^3} - \frac{\mu_2 y}{r_2^3} \qquad (7)$$

Here, terms with a single dot are velocities and those with two dots are accelerations. The terms $2\dot{y}$ in Equation (6) and $-2\dot{x}$ in Equation (7) are the respective Coriolis acceleration components obtained from Equation (5). These two terms do not vanish even at the Lagrangian points and they cause an oscillatory rolling motion called *libration* especially around L4 and L5. As this is an initial value problem (IVP) each orbit is started using a selected set of initial positions and velocities [3, 8]. The orbit integration over a suitable period is carried out using either a fourth order Runge-

Kutta scheme or one of python scipy library functions such as odeint() or dopri5() for more accurate computation.

We start with an illustration in Figure 9 of the possible tadpole shaped libratory orbits of hypothetical dust particles or asteroids around the $L_4$ and $L_5$ points in our own Earth-Moon system which has a mass ratio of 81.3. The orbits are traced out by dots whose spacing varies with the speed of the asteroid. At both the ends of the tadpole orbit this speed is a minimum and hence the dots appear to get much closer there. This would imply that had real asteroids been present they would spend more time there, then pick up speed as they moved towards the other end of the tadpole orbit and slow down again at the other end. In the real non-inertial situation we should remember that the particle is also orbiting the Earth with the same speed as the Moon and so its actual velocity is the vector sum of its orbital velocity and the velocity in its tadpole orbit around the $L_4$ or $L_5$ point. While this is true for the minor body in any circular restricted 3 body system the period of its libration alone exceeds the orbital period by a few multiples.
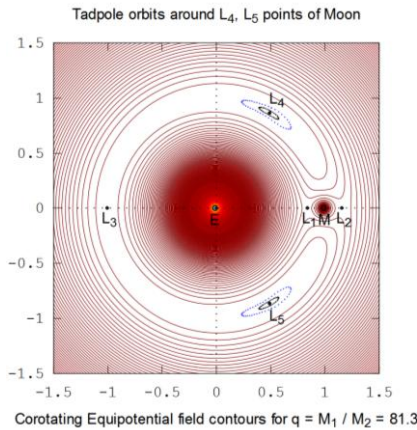


Fig. 9. A pair of tadpole shaped libratory orbits of an asteroid around each equilateral Lagrangian point $L_4$ and $L_5$ is shown here although no such objects are known for the Earth-Moon system. This figure has a scale of 384,000 km/unit.

We now illustrate a similar situation in Figure 10 showing a pair of Trojan asteroid orbits around the $L_4$ and $L_5$ points each of the Sun-Jupiter system. Here the spacing of dots reflects the variation in the speed of a Trojan in its tadpole orbit and the clustering of dots at the pointed end directed

toward $L_3$ indicates that the speed is a minimum there. If a large number of Trojans with same orbital parameters were to be scattered along the orbit then they would cluster around the pointed end. If the outer tadpole orbit had been longer it would have resulted in a horse-shoe shaped orbit around all the three points $L_4$, $L_3$ and $L_5$. The period of the outer tadpole orbit has been calculated as 223 years whereas that of the inner tadpole orbit is 151 years. For a very small orbit in the immediate vicinity of the Lagrangian point, the "tadpole" becomes almost an ellipse, with a limiting period for an infinitesimally small orbit of 147.4 years. Since the Trojans share with Jupiter the same period of revolution around the Sun we can say that they are in a **1:1** orbital resonance.
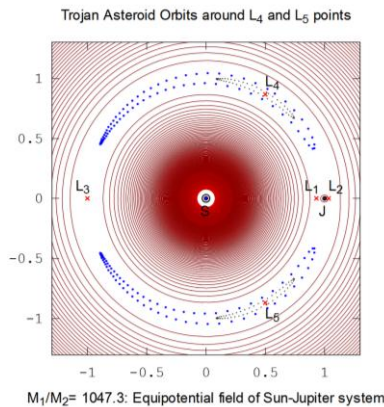


Fig. 10. A pair of tadpole shaped Trojan asteroid orbits around $L_4$ and a mirror image pair of Trojan asteroid orbits around the $L_5$ relative to the planet. The figure has a scale of 5.2 AU/unit.

There is a group of asteroids known as Hildas, after their eponymous member (153) Hilda, which are characterized by orbits whose periods are about two-thirds of that of the planet Jupiter. We show in Figure 11 the ideal stable orbit of a Hilda asteroid starting from its perihelion position when collinear with the Sun and Jupiter. In Figure 12 we show the positions of 790 of these asteroids at a particular instant of time, January 1, 2009, relative to the planet Jupiter. It is seen that they are all situated around a triangle, with particular concentrations around the $L_3$, $L_4$ and $L_5$ points of the Sun-Jupiter system. For the Sun-Jupiter system, the mass ratio $q$ is large (1047.3), and $L_3$ then forms approximately an equilateral triangle with $L_4$ and $L_5$. We can understand the distribution of the Hilda asteroids by looking at their orbits

40

referred to a rotating reference frame in which Jupiter is stationary. The orbits of these asteroids have periods equal to two-thirds of that of Jupiter and with several eccentricities, referred to an inertial reference frame as well as to the rotating reference frame.   In the latter frame they all have equilateral triangle symmetry (symmetry of the type known in group theory as $C_{3v}$ symmetry).      In particular, Hilda itself (and indeed most of the members of the Hilda family) has an eccentricity of about 0.1.   We can imagine the orbit of a Hilda by thinking of a particle sliding on the gravitational-centrifugal potential surface and lurching from one equilateral Lagrangian point to the next.   At each of $L_3$, $L_4$ and $L_5$, the Hilda is at an aphelion of its orbit; it is moving slowly there and spends a lot of time near the Lagrangian point, where its potential energy is large.   Then it hastily and briefly slips below the rim of the solar gravitational well, and scuttles rapidly up to the next equilateral Lagrangian point.  Because of this motion, it is easy to see why, if you take an instantaneous snapshot of the positions of all the Hildas at some arbitrary moment of time, all of them will be strung out along the "Hilda triangle", but with particular concentrations at the Lagrangian (aphelion) points, where they are moving slowest and spending most of their time.

Many asteroids exhibit a tendency to oscillate about a Lagrangian point or slide from one Lagrangian point to the next and back. As stated earlier this is referred to as a *libration* and so the Lagrangian points themselves are also termed as *libration* points. A *libration* cycle is a complete oscillation about the libration points concerned. When any Hilda group asteroid starts some distance away from its perihelion position its triangle orbit oscillates around this position (and the three points $L_3$, $L_4$ and $L_5$) with amplitude of about 40 degrees which constitutes its *libration* cycle and the period is known to be 270 years. This cycle is spread over nearly 23 orbits of Jupiter.
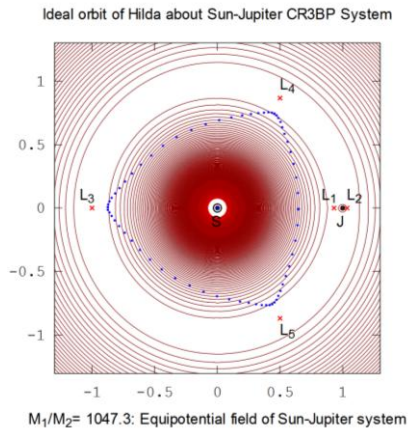
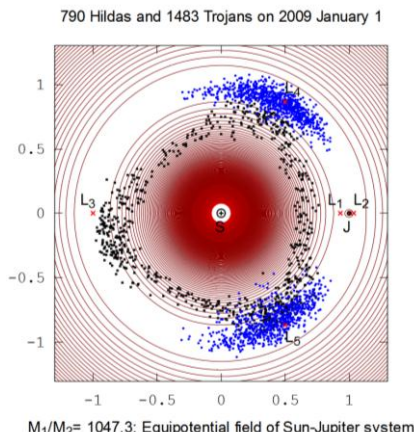Fig. 11. Ideal non-librating orbit of a Hilda group asteroid starting from its collinear perihelion point.



Fig. 12. This diagram shows the positions of 790 Hildas (black dots) in their orbits clustering around $L_3$, $L_4$ and $L_5$ points, 1483 Trojans (blue dots) clustering around the two equatorial Lagrange points $L_4$ and $L_5$ of Jupiter are shown as on 2009 January 1 from data kindly made available by Prof. Aldo Vitagliano, University of Napoli Federico II, Italy. An animated version of this figure can be seen at [7]. All Hildas move in equilateral triangular orbits similar to that shown in Figure 11 and all Trojans execute tadpole orbits similar to those in Figure 10 as well as horse shoe shaped libratory orbits.

We show in Figure 13 the ideal non-librating orbit of Thule whose orbital period bears a ratio of ¾ with that of Jupiter. Thus the orbit looks like a square with its edges rounded off. We next show how the well known *libration* cycle of Pluto develops around the co-rotating Sun-Neptune system in the same CR3BP approximation which here also neglects its large inclination with the ecliptic. Pluto's orbital period of 248.43 years
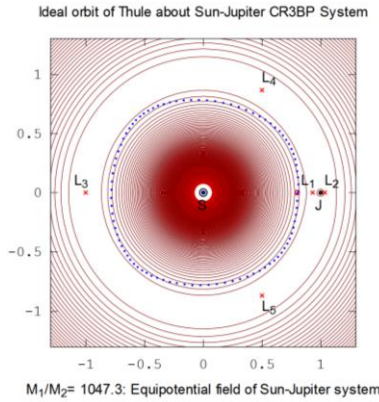
Fig. 13. Here the ideal non-librating orbit of Thule is shown starting from its perihelion position between the Sun and Jupiter. The scale of the figure is also 5.2 AU/unit.

locks it into an exact resonance of **3:2** with Neptune's orbital period of 165.62 years. As Pluto has a large eccentricity of 0.247 compared to Neptune's 0.008 (neglected here), this dwarf planet, as the current IAU classification of Pluto goes, comes closer to the Sun than Neptune. Thus we see in Figure 14 two complete orbits of Pluto which means that Neptune would have done three complete orbits during this period of 497 years which constitutes one basic cycle. The spacing between the dots representing Pluto's orbit show its speed to be the lowest near its perihelion point located near $L_4$ at top left. Pluto can be seen to commence its *libration* from this point. The next basic cycle with two orbits of Pluto is similar but the figure is now slightly rotated by about 3.8 degrees anti-clockwise toward the ordinate. This drawing also indicates that Pluto never approaches Neptune closer than about 17 AU.

The last Figure 15 shows the situation after Pluto has completed 20 basic cycles and 9940 years elapse. Now the first basic cycle has swung by 76 degrees anti-clockwise to the left. Pluto is slightly to the right of $L_5$ in this figure and it has thus completed half a *libration* cycle. It is now starting its reverse (that is, clockwise) swing of another 20 basic cycles or 76 degrees over a further period of 9940 years to reach the same vicinity of $L_4$ point it started from. Thus a *libration* cycle of Pluto takes about 19880 years (sidereal time) in the co-rotating frame of the Sun-Neptune system.
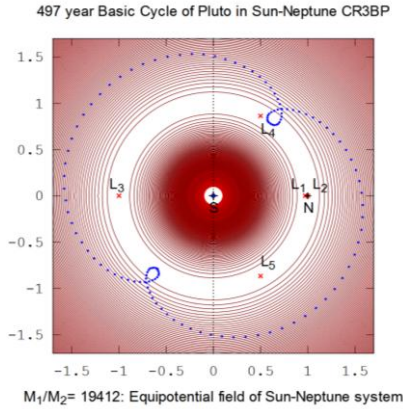
Fig. 14. Neptune (labelled N) is located to the right of the Sun (labelled S) and the scale of this figure is 30.16 AU/unit. Pluto starts from L4 , completes two orbits traced out by dots spaced according to the speed of the planetoid and returns to the same point in 497 years.
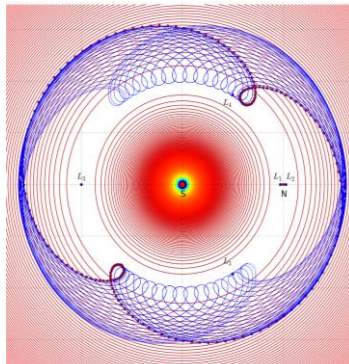


Fig. 15. Pluto is near the trailing point L5 now after completing 20 basic cycles. Note that the basic cycle of Figure 14 is identified here as a string of red dots (Figure drawn using Pylab software.)

## 4. Figure of Eight Orbits of Three Bodies of Equal Mass

We shall now briefly consider the recent discovery of a surprisingly simple and stable periodic orbit for the Newtonian problem of three equal masses in a plane whose existence was rigorously proved [9]. This three body orbit has zero total angular momentum and a very rich symmetry pattern. The most surprising feature is that the three bodies chase each other around a fixed eight-shaped

44

curve visiting by turns every "Euler configuration" in which one of the bodies sits at the midpoint of the segment defined by the other two as shown in Figure 16. Each body traverses a one third section of the orbit in a time T/3 where period T is 6.32591398 units. The starting position of each body is marked by a large circle (colored red, blue and green respectively). These are joined together by a straight line (dashed cyan). These positions are based on initial position coordinates while each body starts its orbit along the directed arrow shown with its initial velocities as given in [9] and are also reproduced here as a scaled planar position and velocity array [x0, y0, vx0, vy0] to enable dynamic simulation by interested readers:

Body No.1: [ 0.97000436, -0.24308753,  0.466203685, 0.43236573 ]

Body No.2: [-0.97000436,  0.24308753,  0.466203685, 0.43236573 ]

Body No.3: [     0.0,            0.0,      -0.93240737, -0.86473146 ]

In this scaled system, G = 1 and each body has unit mass. The figure-of-eight orbit is so gracefully executed that the motion is called choreographic since each body moves periodically in a single closed orbit. The small dots in front of each body position along its orbit are the successive positions of the respective bodies spaced at **equal time** intervals of T/36 and hence they show the speed of the body along its orbit. In Figure **17** the complete orbit travelled by each body in time T is shown. As each body moves 3 dots further along (a time T/12 later) it occupies the vertices of an isosceles triangle formed by dashed blue lines. This is a triangular configuration of the three bodies. The Euler configuration appears again (dotted cyan) after moving three dots further on. Then a mirror image of the first triangular configuration appears (dotted blue) after each body moves three dots further along. In all such recurring configurations the bodies take their turn at every available position. Orbits of this type exist only in the domains of theoretical mechanics and computational simulation but there appears to be little chance of an actual discovery by ground based and spacecraft borne astronomical instruments.
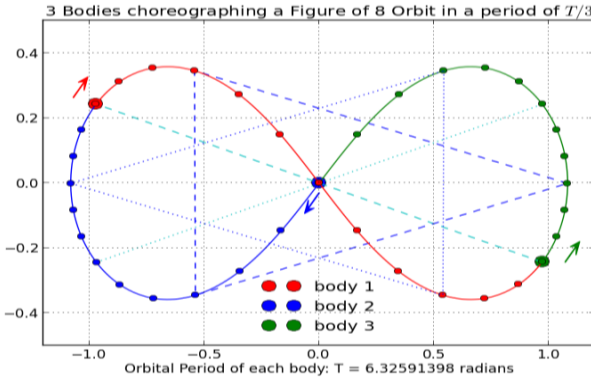
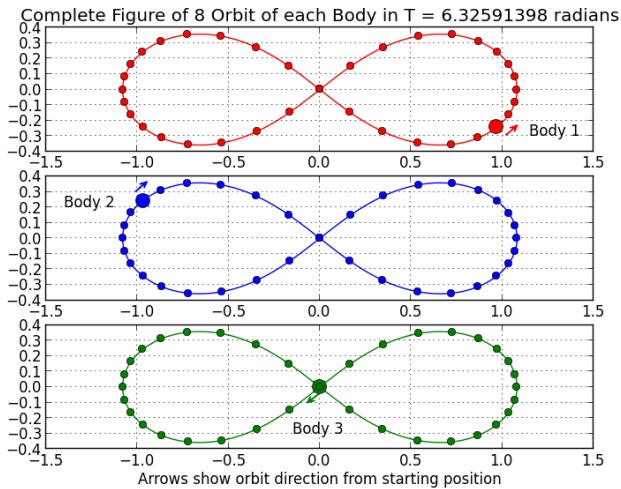Fig. 16. Choreographed figure of 8 orbit of three bodies of equal mass.



Fig. 17. The complete orbit of each of the three masses is shown here.

## 5. Conclusion

We have shown that a variety of interesting minor body orbits exist which are influenced by many two-body systems dominated by the sun and a planet. It is clear that while the solar system is really a complex n-body problem it admits many levels of simplification. At the basic level we are familiar with many two body systems whose

46

dynamics can be understood in terms of the well known Kepler's laws of motion. Now we have shown here that at the next level of simplification the circular restricted three body systems offer a means of computing many types of observable minor body orbits. Among the many minor bodies of interest the Trojans are a large group of asteroids trapped close to the equatorial Lagrangian points of the associated planet.As of January 2014, according to [4], 5946 Trojan asteroids have been identified. These comprise 1 Sun-Earth Trojan, 5 Sun-Mars Trojans, 5930 Sun-Jupiter Trojans, 1 Sun-Uranus Trojan and 9 Sun-Neptune Trojans. It has been a challenging research task to discover these objects since they are faint, far away and need to be identified in a dense field of similar background objects. Many more Trojans in many of the sun-planet systems and also of the planet-moon systems in our solar system await discovery and we invite younger readers to take up this challenging research opportunity. A great deal of information including possible technological applications may be found in [2, 5, 7]. Many techno-commercial ventures are already active seeking to drag multi-kilo-ton sized asteroids orbiting near earth (NEO) to the inner Lagrangian point $L_1$ of the Earth-Moon system and mine them for valuable minerals.

## Acknowledgment

## References

[1]. J. B. Tatum, Lecture Notes on Celestial Mechanics, Chapter16, 2014.

[2]. CCAR Project Geryon homepage: http://ccar.colorado.edu/geryon/

[3]. P. Hellings, Astrophysics with a PC, Willmann-Bell Inc., USA, 1994.

[4]. IAU MPC homepage: http://www.minorplanetcenter.net/iau /lists/Trojans.html

[5]. Shane Ross homepage:   http://www2.esm.vt.edu/~sdross/

[6]. Tatum homepage :  http://orca.phys.uvic.ca/~tatum

[7]. A. Vitagliano, home page:   http://main.chemistry.unina.it/ ~ alvitagl/

[8]. P. W. Sharp, A Collection of R3B Test Problems, www.math.auckland. ac.nz /~sharp (2001).

[9]. **A.** Chenciner and R. Montgomery, A remarkable periodic solution of the three body problem in the case of equal masses, Annals of Mathematics, 152, pp881-901 , 2000.

[10].        http://www.bdl.fr/Equipes/ASD/preprints/prep.2000/ huit.pdf

# Appendix A

## Biographical sketch of Jeremy B. Tatum



Dr. Tatum is a retired Professor of Physics and Astronomy at the University of Victoria, Canada. Much of his research work has involved molecular spectroscopy - in particular the theory of the intensities of spectrum lines and the determination of molecular abundances in stars and comets. He has served on the Meteorites and Impacts Advisory Committee to the Canadian Space Agency, and has achieved immortality in the form of the asteroid (3748) Tatum. He has made some contributions to the study of the Lepidoptera of Vancouver Island. A matter of family pride for him is that an ancestor taught natural philosophy in a dozen lectures to Michael Faraday during 1812. [ This is mentioned in page 32  of the well known book, Introduction to Modern Physics, by Richtmyer, Kennard and Cooper, TMH edition, 1997]. He can be contacted at jtatum@uvic.ca. The second author Dr. Anandaram was his doctoral student at the University of Victoria.